Tuning the size of poly(butylene oxide) nanoparticles by microfluidic-assisted nanoprecipitation

Lachlan Alexander,[a,b,c#] Marat Mamurov,[a,c#] Hiba Khelifa,[a,d#] Nicolas Illy,[d] Philippe Guégan,[d] Christophe M. Thomas,[a] Samuel Hidalgo-Caballero,[c,e] Joshua D. McGraw,[c,e*] and Kawthar Bouchemal [a*]

a. Chimie ParisTech, PSL University, CNRS, Institut de Recherche de Chimie Paris, 75005 Paris, France.

b. Monash University, Clayton, Australia.

c Gulliver, CNRS, ESPCI Paris, Université PSL, 75005 Paris, France

d Sorbonne Université, CNRS, Institut Parisien de Chimie Moléculaire, IPCM, F-75005 Paris, France

e Institut Pierre Gilles de Gennes (IPGG), ESPCI Paris, Université PSL, 75005 Paris, France

[#] Equally contributing first authors

* Corresponding authors

kawthar.bouchemal@chimieparistech.psl.eu

joshua.mcgraw@espci.fr

1. Fabrication of PDMS chips with variable geometries and dimensions

PDMS microfluidic chips were successfully fabricated using a Sylgard™ 184 elastomer kit, glass microscope slides, and a plasma cleaner, employing an efficient and sustainable method that enabled the rapid production of multiple chips. In one approach, chips with variable geometries and dimensions were fabricated with 50 g of PDMS/crosslinker mixture, while another method produced over 15 chips from six reusable silicon wafers using the same quantity of materials. Both techniques ensured a convenient and long-lasting chip supply throughout the experiment.

A critical step in the fabrication process was degassing the PDMS mixture to eliminate trapped air bubbles that could compromise the microfluidic channels' integrity. Degassing was conducted in a vacuum chamber, where both the strength of the vacuum and the ambient temperature played pivotal roles. Higher temperatures risked premature curing, trapping air bubbles and leading to chip failure. However, stronger vacuum settings successfully removed air, while even weaker vacuum systems were effective if used at lower room temperatures.

The plasma cleaning step was essential for fabricating the chips and ensuring their experimental reproducibility. Exposure to air plasma oxidized the surface methyl groups on both the PDMS and the glass slides, converting them into silanol groups. When the two components came into Aqact, spontaneous and irreversible siloxane bridges formed, firmly bonding them together. This step also functionalized the chip surface with silanol groups, improving its wetting properties for polar liquids and ensuring consistent flow through the channels.[1]

Proper plasma treatment was crucial to the device's structural stability, especially under higher flow pressures. Insufficient treatment, as demonstrated using an alternative plasma device, resulted in devices detaching from the glass slides under increased flow velocities. The optimal plasma treatment allowed the chips to withstand these pressures reliably. Additionally, curing temperature significantly affected the chip’s performance. Chips cured at 70 °C for 3 hours achieved optimal flexibility and durability, while those cured at 90 °C for 1 hour became rigid and prone to tearing under high-pressure flow conditions.

These chips exhibited excellent long-term stability, maintaining experimental reproducibility for at least six weeks in storage.

2. Design of poly(butylene oxide) nanoparticles via microfluidic-assisted nanoprecipitation in hydrodynamic flow focusing (Ψ-geometry)

Table S1: Effect of poly(butylene oxide) concentration ([PBO]) on nanoparticle size and PDI. Nanoparticles were obtained using a Ψ-geometry microfluidic device without junction with 100 × 100 µm channel dimensions. *R* was maintained at 0.06 (1:15) while total flow (*TF*) varies from 32 to 96 µL min^{-1}. Channel length l_1 was maintained at 10 mm. The PBO concentration was varied as 1.87, 3.75, 7.5, and 15 mg mL^{-1}. The kinematic viscosities of the aqueous phase, organic phase, and nanoparticle suspension were 1.077, 2.044, and 1.51 10^{-6} m^2 s^{-1}. (*n* = 3)

Flow parameters after mixing				***d_h** z-average (nm) and (*PDI*)**			
TF **(µL min^{-1})**	***u_{mix}*** **(mm s^{-1})**	***τ_{Res}*** **(ms)**	***Re_{mix-C}***	**[PBO] 15 mg mL^{-1}**	**[PBO] 7.50 mg mL^{-1}**	**[PBO] 3.75 mg mL^{-1}**	**[PBO] 1.87 mg mL^{-1}**
32	53.33	188	3.51	593 ± 84 (*0.55 ± 0.02*)	370 ± 18 (*0.50 ± 0.09*)	237 ± 9 (*0.41 ± 0.02*)	173 ± 3 (*0.24 ± 0.00*)
64	106.67	94	7.02	568 ± 121 (*0.56 ± 0.04*)	370 ± 19 (*0.48 ± 0.04*)	234 ± 7 (*0.39 ± 0.01*)	166 ± 4 (*0.25 ± 0.01*)
96	160.00	63	10.53	564 ± 43 (*0.63 ± 0.04*)	278 ± 19 (*0.41 ± 0.04*)	223 ± 10 (*0.33 ± 0.03*)	147 ± 2 (*0.23 ± 0.00*)

Channel dimensions in the aqueous and the organic phases before mixing were w_3 = 75 µm and $h_{1\text{-}100}$ = 100 µm. Channel cross sections before mixing were $A_{B\text{-}100}$ = 7.5 × 10^3 μm^2. Channel dimensions after mixing were $w_{1\text{-}100}$ = 100 µm. Channel cross sections after mixing $A_{A\text{-}100}$ = 10^4 μm^2.

Notations: The Reynolds number of the organic phase, $Re_{mix\text{-}C}$*:* The Reynolds number upon mixing the aqueous and the organic phases in the channel, mixing time τ_{mix} = 3.15 ms.

3. Optimization of flow parameters

Table S2: Flow parameters for Ψ-geometry without junction 100 × 100 µm channel dimensions. *R* was changed as 0.1 (1:10), 0.08 (1:12), 0.06 (1:16), and 0.05 (1:20), and the *TF* varies from 13 to 147 µL min^{-1}. Channel length l_1 was maintained at 10 mm. The poly(butylene oxide) concentration was maintained at 3.75 mg mL^{-1}. The kinematic viscosities of the aqueous phase, organic phase, and nanoparticle suspension were 1.077, 2.044, and 1.51 10^{-6} m^2 s^{-1}. (n = 3)

R	Flow parameters before mixing						Flow parameters after mixing						d_h* z-average (nm) and (*PDI*)
	Aqueous phase			Organic phase									
	Q_{Aq} (µL min^{-1})	u_{Aq} (mm s^{-1})	Re_{Aq}	Q_{Org} (µL min^{-1})	u_{Org} (mm s^{-1})	Re_{Org}	*TF* (µL min^{-1})	u_{mix} (mm s^{-1})	τ_{Res} (ms)	$Re_{mix\text{-}C}$	τ_{mix} (ms)	L_{mix} *(mm)*	
0.1	11.82	26.27	1.83	1.18	2.62	0.10	13	21.67	462	1.43	7.53	0.163	380 ± 44 (*0.33 ± 0.05*)
	23.64	52.53	3.66	2.37	5.27	0.19	26	43.33	213	2.85		0.326	328 ± 25 (*0.23 ± 0.07*)
	35.45	78.78	5.48	3.45	7.67	0.28	39	65.00	154	4.28		0.489	306 ± 12 (*0.30 ± 0.14*)
0.08	16.61	36.91	2.57	1.38	3.07	0.11	19	30.00	333	1.98	5.39	0.162	367 ± 15 (*0.44 ± 0.05*)
	35.07	77.93	5.42	2.92	6.49	0.24	38	63.33	158	4.17		0.341	282 ± 9 (*0.38 ± 0.02*)
	52.61	116.91	8.12	4.38	9.73	0.36	57	95.00	105	6.26		0.512	277 ± 9 (*0.36 ± 0.02*)
0.06	30.11	66.91	4.66	1.88	4.18	0.15	32	53.33	188	3.51	3.15	0.168	237 ± 9 (*0.41 ± 0.02*)
	60.23	133.84	9.31	3.76	8.36	0.31	64	106.67	94	7.02		0.336	234 ± 7 (*0.39 ± 0.01*)
	90.35	200.78	13.97	5.64	12.53	0.46	96	160.00	63	10.53		0.504	223 ± 10 (*0.33 ± 0.03*)
0.05	46.67	103.71	7.22	2.33	5.18	0.19	49	81.67	122	5.38	2.07	0.169	242 ± 22 (*0.43 ± 0.06*)
	93.33	207.40	14.43	4.67	10.38	0.38	98	163.33	61	10.75		0.337	235 ± 9 (*0.43 ± 0.04*)
	140.00	311.11	21.65	7.00	15.56	0.57	147	245.00	41	16.13		0.506	203 ± 3 (*0.35 ± 0.03*)

Channel dimensions in the aqueous and the organic phases before mixing were w_3 = 75 µm and $h_{1\text{-}100}$ = 100 µm. Channel cross sections before mixing were $A_{B\text{-}100}$ = 7.5 × 10^3 µm^2. Channel dimensions after mixing were $w_{1\text{-}100}$ = 100 µm. Channel cross sections after mixing $A_{A\text{-}100}$ = 10^4 µm^2.

Notations: Q_{Aq}: flow rate of the aqueous phase, u_{Aq}: velocity of the aqueous phase, Re_{Aq}: The Reynolds number of the aqueous phase, Q_{Org}: flow rate of the organic phase, u_{org}: velocity of the organic phase, Re_{Org}: The Reynolds number of the organic phase, $Re_{mix\text{-}C}$: The Reynolds number upon mixing the aqueous and the organic phases in the channel; τ_{mix} is the mixing time and L_{mix} is the mixing distance corresponding to the distance required for complete mixing.

4. Nanoparticle size versus total flow

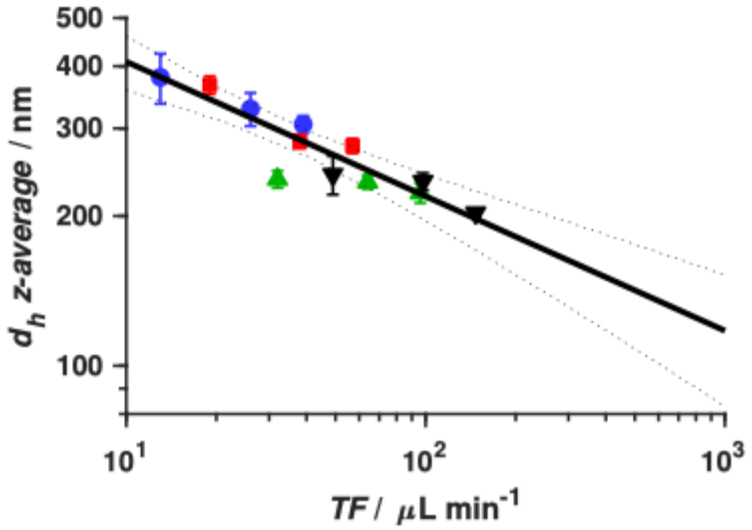

Fig. S1. Nanoparticle size versus total flow (*TF*). The solid line is the best fit to a power-law relation $\boldsymbol{d_h = A(TF)^{-\alpha}}$ with $\boldsymbol{A = 800 \pm 300}$ nm $\left(\text{min } \mu\text{L}^{-1}\right)^{\boldsymbol{\alpha}}$ and $\boldsymbol{\alpha = 0.3 \pm 0.1}$. The errors account for a 95% confidence interval, and the dotted lines similarly represent a 95% confidence band.

5. Optimization of microfluidic geometry

Table S3: Flow parameters for T- and Ψ-geometry without junction 100 × 100 µm, 40 × 40 µm, and 20 × 20 µm channel dimensions. *R* was maintained at 0.06. Channel length l_1 was maintained at 10 mm. The poly(butylene oxide) concentration was maintained at 1.875 mg mL^{-1}. The kinematic viscosities of the aqueous phase, organic phase, and nanoparticle suspension were 1.077, 2.044, and 1.51 10^{-6} m^2 s^{-1}. (n = 3)

$w_1 \times h_1$ (µm)	Flow parameters before mixing						Flow parameters after mixing					d_h* *z*-average (nm) and (PDI)	
	Aqueous phase			Organic phase								T-geometry	Ψ-geometry
	Q_{Aq} (µL min^{-1})	u_{Aq} (mm s^{-1})	Re_{Aq}	Q_{Org} (µL min^{-1})	u_{Org} (mm s^{-1})	Re_{Org}	TFR (µL min^{-1})	u_{mix} (mm s^{-1})	τ_{Res} (ms)	$Re_{mix\text{-}C}$	τ_{mix} (ms)		
100 × 100	30.12	66.93	4.66	1.88	4.18	0.15	32	53.33	188	3.51	3.15	354 ± 80 (0.280 – 0.486)	151 ± 3 (0.232 – 0.257)
	60.23	133.84	9.31	3.77	8.38	0.31	64	106.67	94	7.02		358 ± 82 (0.273 – 0.415)	163 ± 6 (0.212 – 0.256)
	90.35	200.78	13.97	5.64	12.56	0.46	96	160.00	63	10.53		403 ± 92 (0.312 – 0.511)	149 ± 12 (0.214 – 0.284)
40 × 40	30.12	167.33	11.64	1.88	10.44	0.38	32	333.33	30	8.78	0.5	556 ± 188 (0.437 – 0.671)	116 ± 3 (0.278 – 0.282)
	60.23	334.61	23.29	3.77	20.94	0.77	64	666.67	15	17.56		455 ± 272 (0.380 – 0.815)	179 ± 53 (0.293 – 0.427)
	90.35	501.94	34.93	5.65	31.39	1.15	96	1000.00	10	26.34		267 ± 18 (0.566 – 0.625)	226 ± 52 (0.364 – 0.454)
20 × 20	1.88	20.89	1.45	0.12	1.33	0.05	2	83.33	120	1.10	0.13	188 ± 15 (0.246 – 0.366)	137 ± 7 (0.221 – 0.311)
	3.76	41.78	2.91	0.24	2.67	0.10	4	166.67	60	2.19		202 ± 21 (0.290 – 0.414)	92 ± 6 (0.297 – 0.424)
	7.53	83.67	5.82	0.47	5.22	0.19	8	333.33	30	4.39		424 ± 123 (0.401 – 0.553)	66 ± 12 (0.221 – 0.311)

Channel dimensions in the aqueous and the organic phases before mixing were w_3 = 75 µm and $h_{1\text{-}100}$ = 100 µm, $h_{1\text{-}40}$ = 40 µm, or $h_{1\text{-}20}$ = 20 µm. Channel cross sections before mixing were $A_{B\text{-}100} = 7.5 \times 10^3$ µm², $A_{B\text{-}40} = 3.0 \times 10^3$ µm² and $A_{B\text{-}20} = 1.5 \times 10^3$ µm². Channel dimensions after mixing were $w_{1\text{-}100}$ = 100 µm, $w_{1\text{-}40}$ = 40 µm, or $w_{1\text{-}20}$ = 20 µm. Channel cross sections after mixing $A_{A\text{-}100} = 10^4$ µm², $A_{A\text{-}40} = 1.6 \times 10^3$ µm², or $A_{A\text{-}20} = 4 \times 10^2$ µm².

Notations: Q_{Aq}: flow rate of the aqueous phase. u_{Aq}: velocity of the aqueous phase. Re_{Aq}: The Reynolds number of the aqueous phase. Q_{Org}: flow rate of the organic phase. u_{Org}: velocity of the organic phase. Re_{Org}: The Reynolds number of the organic phase. $Re_{mix\text{-}C}$: The Reynolds number upon mixing the channel's aqueous and organic phases.

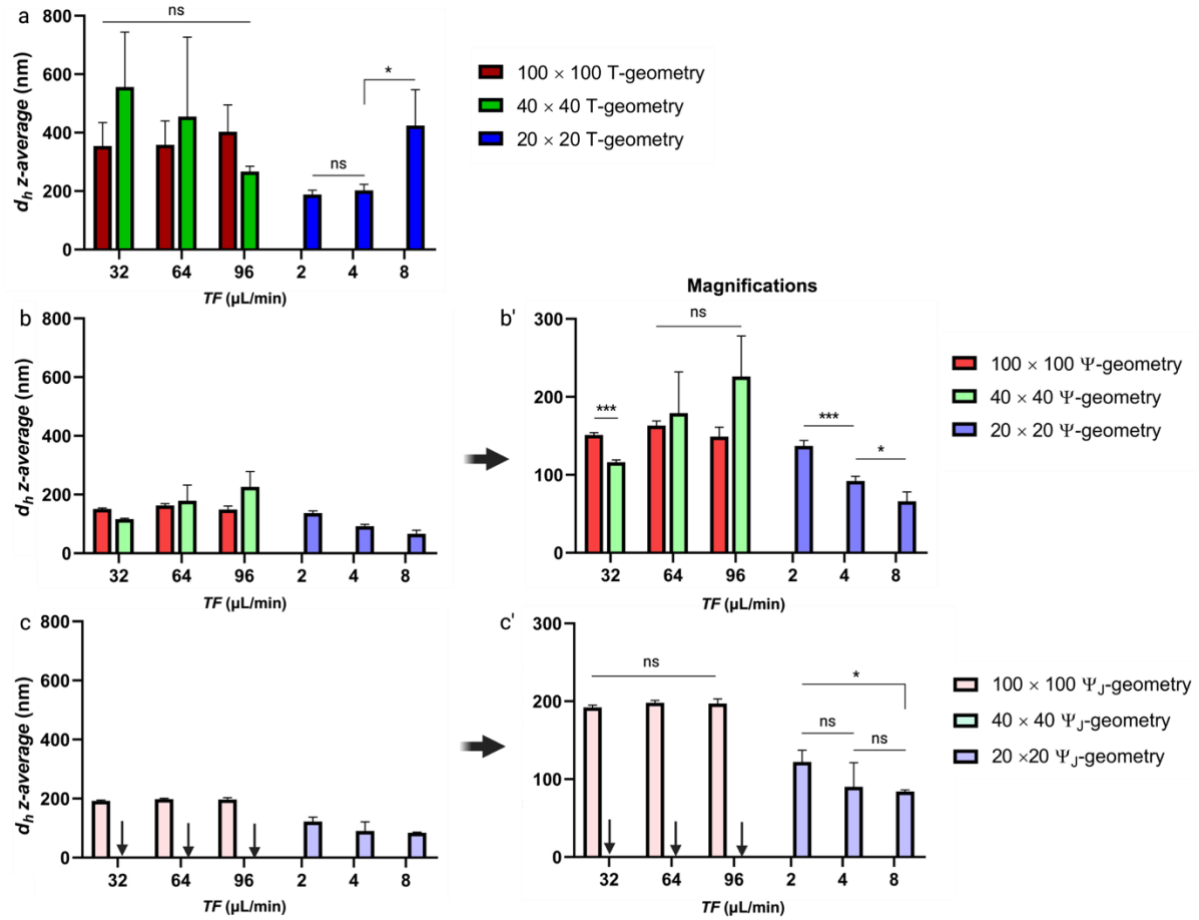

Fig. S2. Effect of channel geometry and total flow (*TF*) on mean hydrodynamic size of PBO nanoparticles. *R* was maintained at 0.06. The poly(butylene oxide) concentration was 1.875 mg mL^{-1}. Statistical analysis was performed with two-way ANOVA followed by Tukey's post-test. One, two, three, and four asterisks denote a *p*-value < 0.05, < 0.01, < 0.001, and <0.0001, respectively. "ns" denote a non-significant difference. (*n* = 3)

Table S4: Effect of microfluidic geometry and dimensions on PBO nanoparticle mean hydrodynamic diameters. Nanoparticles were obtained by using a Ψ_J-geometry with 100 × 100 μm or 20 × 20 μm channel dimensions. *R* was maintained at 0.06. Channel length l_1 was maintained at 10 mm. The poly(butylene oxide) concentration was maintained at 1.875 mg mL^{-1}. The kinematic viscosities of the aqueous phase, organic phase, and nanoparticle suspension were 1.077, 2.044, and 1.51 10^{-6} m^2 s^{-1}. (*n* = 3)

$w_1 \times h_1$ ($w_2 \times l_2$) (μm)	Flow parameters before mixing						Flow parameters after mixing of the aqueous and organic phases				d_h* *z*-average (nm) and (PDI)
	Aqueous phase			Organic phase							
	Q_{Aq} (μL min^{-1})	u_{Aq} (mm s^{-1})	Re_{Aq}	Q_{Org} (μL min^{-1})	u_{Org} (mm s^{-1})	Re_{Org}	TFR (μL min^{-1})	u_{mix} (mm s^{-1})	τ_{mix} (ms)	$Re_{mix\text{-}C}$	
100 × 100 (20 × 30)	30.12	66.93	4.66	1.88	4.18	0.15	32	53.33	3.15	3.51	192 ± 3 (0.187 – 0.246)
	60.23	133.84	9.31	3.77	8.38	0.31	64	106.67		7.02	198 ± 3 (0.229 – 0.342)
	90.35	200.78	13.97	5.64	12.56	0.46	96	160.00		10.53	197 ± 6 (0.199 – 0.311)
20 × 20 (4 × 6)	1.88	20.89	1.45	0.12	1.33	0.05	2	83.33	0.13	1.10	122 ± 15 (0.166 – 0.265)
	3.76	41.78	2.91	0.24	2.67	0.10	4	166.67		2.19	90 ± 31 (0.160 – 0.29)
	7.53	83.67	5.82	0.47	5.22	0.19	8	333.33		4.39	84 ± 2 (0.192 – 0.252)

Channel dimensions in the aqueous and the organic phases before mixing were w_3 = 75 μm and $h_{1\text{-}100}$ = 100 μm or $h_{1\text{-}20}$ = 20 μm. Channel cross sections before mixing were $A_{B\text{-}100}$ = 7.5 × 10^3 μm^2 and $A_{B\text{-}20}$ = 1.5 × 10^3 μm^2. Channel dimensions after mixing were $w_{1\text{-}100}$ = 100 μm or $w_{1\text{-}20}$ = 20 μm. Channel cross sections after mixing $A_{A\text{-}100}$ = 10^4 μm^2 or $A_{A\text{-}20}$ = 4 × 10^2 μm^2. Channel cross sections after mixing were $A_{A\text{-}100}$ = 10^4 μm^2 or $A_{A\text{-}20}$ = 4 × 10^2 μm^2.

Notations: Q_{Aq}: flow rate of the aqueous phase, u_{Aq}: The velocity of the aqueous phase is calculated according to Eq.3, Re_{Aq}: The Reynolds number of the aqueous phase is calculated according to Eq.1, Q_{Org}: flow rate of the organic phase, u_{Org}: The velocity of the organic phase, Re_{Org}: The Reynolds number of the organic phase, $u_{mix\text{-}J}$: velocity upon mixing the aqueous and the organic phases in the junction, $Re_{mix\text{-}J:}$ The Reynolds number upon mixing the aqueous and the organic phases in the junction, $Re_{mix\text{-}C:}$ The Reynolds number upon mixing the aqueous and the organic phases in the channel.

For size measurements: *PDI*: polydispersity index. *Y*-intercept > 0.866.

Zeta potential (ζ) was equal to 0.02 ± 0.35 mV. * z-average determined by DLS without dilution.

6. Protocol for density measurement of the aqueous and the organic phases

In this section, we detailed the protocols for measuring the density of the aqueous and organic phases. The aqueous phase is composed of a mixture of water and Tween® 80, used as a water-soluble surfactant. The organic phase is composed of a solution of poly(butylene oxide) and a surfactant that is soluble in ethanol (Span® 80). Controls without surfactants were also prepared.

6.1. Materials

Tween® 80, Span® 80, ethanol (>99.5%), and mineral oil (for molecular biology, M5904, 0.84 g mL^{-1} at 25 °C) were purchased from Sigma-Aldrich, Saint Quentin Fallavier, France). PBO was synthesized as reported in the main text. Milli-Q® water was used for all the experiments (Resistivity 18.2 MΩ.cm at 21 °C, Millipore purification system, Millex, SLAP 0225, Millipore, France). Ethanol and water were filtered through a 0.45 µm filter before use.

6.2. Equipment

HAPC pump controller; 11 Pico Plus Elite Pump; Hamilton glass syringes 5 and 10 mL; B-190TBPL Microscope Optika with screen; Microfluidic chips (PDMS chips with a Y junction 600 µm width and 30 µm height); 0.5 mm silicone tubing 0.5 mM ID; 23G stainless steel microfluidic adaptors 0.5 mm ID; glass vials with cap 3 mL (to measure the density).

6.3. Methods

6.3.1. Phase preparation

Aqueous and organic phases were prepared, as reported in the main text. Below, we report the composition of each phase. For the organic phase, PBO concentration was 1.875 mg mL^{-1}, Span® 80 (2 mg mL^{-1}), and ethanol. The aqueous phase was composed of Tween® 80 (3 mg mL^{-1}) in MilliQ water.

6.3.2. Density measurement

- P1000 micropipette is adjusted to 1 mL volume
- The glass vial was weighed, 1 mL of the solution was added to the vial, and the weight was noted.
- The experiment is performed 3 times 1 mL of the solution is weighted for all solutions and noted
- The density (ρ) is calculated by dividing the average mass (m) by the average volume (V) according to Eq. S1.

$$\rho = \frac{m}{V} \quad Eq.S1$$

6.3.3. Viscosity measurement

- A Y-geometry PDMS microfluidic chip with the following dimensions was used:
  - The channel width: $w_1 = w_3 = 600$ µm
  - The channel height $h_1 = 30$ µm
  - The channel cross-section: $A = 18 \times 10^3$ µm^2.
- In the typical protocol, the 10 mL Hamilton syringe is filled with mineral oil, which is the reference liquid.

- The 5 mL Hamilton syringe is filled with the liquid whose viscosity needs to be measured
- After the flow rates are set through, the pictures are taken.
- The pictures are analyzed with imageJ and the widths of the phases are measured
- The viscosity is calculated with Eq. S2.

$$\eta = \frac{W\eta_r Q_r}{W_r Q} \qquad \text{Eq. S2}$$

Where:

η is the viscosity of the liquid with unknown viscosity (mPa.s)
W_r is the width of the reference liquid (mineral oil) (µm)
η_r is the viscosity of the reference liquid (mineral oil) (mPa.s)
Q_r is the *TF* of the reference liquid (5 µL min^{-1})
W is the width of the liquid with unknown viscosity (µm)
Q is the *TF* of the liquid with unknown viscosity (µL min^{-1})

- For sample phases, the flow rate increased until the widths of the phases became equal. Those flow rates were 80 µL min^{-1} for the organic phase and 120 µL min^{-1} for the aqueous phase.
- The viscosity of the referent oil is measured using the formula from the viscosity of water with this method.
- The widths of the phases used were almost equal, reducing the error of the system[2].

6.4. Results

6.4.1. Density

Table S5: Density measurement results for organic phases (n = 3).

Phase	Density measurement trials	ρ (kg m^{-3})	Average ρ (kg m^{-3})
Organic phase poly(butylene oxide) /ethanol/Span® 80	Measurement 1	789	788
	Measurement 2	785	
	Measurement 3	790	
Aqueous phase Water/Tween® 80	Measurement 1	980	983
	Measurement 2	983	
	Measurement 3	987	
Nanoparticle suspension of poly(butylene oxide)	Measurement 1	966	985
	Measurement 2	991	
	Measurement 3	998	

6.4.2. Viscosity

Table S6: Viscosity measurement results for the referent oil.

	w_r (μm)	w (μm)	η_r (mPa s)	Q_r (μL min^{-1})	Q (μL min^{-1})	η **(mPa s)**
Mineral oil	270.7	329.3	1.002	130	5	**31.69**
Organic phase (PBO/Span® 80/ethanol)	330.92	266.08	**31.69**	5	80	**1.58**
Aqueous phase (water/Tween® 80)	332.81	267.19	**31.69**	5	120	**1.06**
poly(butylene oxide) nanoparticle suspension	324.38	275.62	**31.69**	5	90	**1.49**

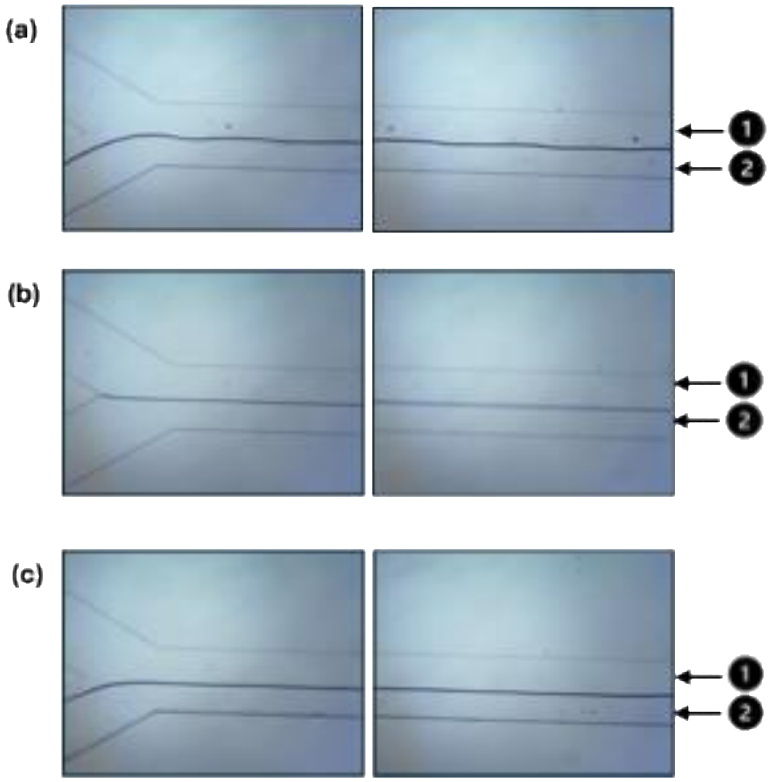

Fig. S3 Typical images of the microfluidic channels of the mineral oil for calibration (a), organic phase (b), and aqueous phase (c). The organic phase is composed of a mixture of poly(butylene oxide) and Span® 80 in ethanol. The aqueous phase is composed of Tween® 80 in water. For each picture, the upper phase (1) corresponds to the mineral oil for calibration, and the lower phase (2) corresponds to the sample. The channel width was 600 μm.

References

1. D. C. Duffy, J. C. McDonald, O. J. Schueller and G. M. Whitesides, *Analytical chemistry*, 1998, **70**, 4974-4984.
2. D. E. Solomon and S. A. Vanapalli, *Microfluidics and nanofluidics*, 2014, **16**, 677-690.